

## Article (refereed) - postprint

---

Formetta, Giuseppe; Prosdocimi, Ilaria; Stewart, Elizabeth; Bell, Victoria.  
2018. **Estimating the index flood with continuous hydrological models:  
an application in Great Britain.**

© IWA Publishing 2018

This version available <http://nora.nerc.ac.uk/519032/>

NERC has developed NORA to enable users to access research outputs wholly or partially funded by NERC. Copyright and other rights for material on this site are retained by the rights owners. Users should read the terms and conditions of use of this material at

<http://nora.nerc.ac.uk/policies.html#access>

**This document is the author's final manuscript version of the journal article, incorporating any revisions agreed during the peer review process. There may be differences between this and the publisher's version. You are advised to consult the publisher's version if you wish to cite from this article.**

**The definitive peer-reviewed and edited version of this article is published in *Hydrology Research* 49 (1) 123-133 (2018).  
[10.2166/nh.2017.251](https://doi.org/10.2166/nh.2017.251) and is available at [www.iwapublishing.com](http://www.iwapublishing.com).**

Contact CEH NORA team at  
[noraceh@ceh.ac.uk](mailto:noraceh@ceh.ac.uk)

# 1 **Estimating the index flood with continuous hydrological models: an** 2 **application in Great Britain.**

3  
4 Giuseppe Formetta<sup>1</sup>, Ilaria Prosdocimi<sup>2</sup>, Elizabeth Stewart<sup>1</sup>, and Victoria Bell<sup>1</sup>

5  
6 <sup>1</sup>Centre for Ecology & Hydrology, Maclean Building, Crowmarsh Gifford, Wallingford OX10 8BB

7 <sup>2</sup>Department of Mathematical Sciences, University of Bath, Claverton Down, Bath BA2 7AY

8  
9 Estimates of peak river discharge are essential for designing and managing hydraulic  
10 infrastructure such as dams, bridges, and flood alleviation schemes. Typically these  
11 are derived for an assigned annual exceedance probability (e.g. the 1 in 100 year  
12 flood), and the provision of accurate estimates is a critical issue in engineering  
13 hydrology, affecting both financial cost and human lives. In the UK, practitioners  
14 typically apply the Flood Estimation Handbook (FEH) statistical method which  
15 estimates the design flood as the product of a relatively frequent flow estimate (the  
16 index flood, IF) and a dimensionless regional growth factor used for estimating peak  
17 flows at higher return periods. For gauged catchments the IF is usually estimated from  
18 observations as the median annual maximum flow which has a two year return period.  
19 For ungauged catchments it is computed through a multiple linear regression model  
20 based on a set of morpho-climatic indices of the basin.

21 While the FEH IF methods provide peak flow estimates that are robust and defensible,  
22 they do not readily take into account catchment or rainfall heterogeneity (important for  
23 large catchments) or the effect of environmental change on river flows. Successful  
24 application to regions outside the UK currently requires a network of good quality, long-

25 term flow gauges to underpin the design flood method, not always present in less  
26 industrialised regions of the world.

27 With the aim of addressing these limitations, we present and assess a methodology  
28 to estimate the IF at national scale using continuous simulation from an area-wide  
29 physically-based hydrological model (Grid-to Grid or “G2G”). The new methodology is  
30 tested across Great Britain and compares well with estimates of the IF at 550 gauging  
31 stations ( $R^2=0.91$ ) and similar performance simulating the annual maxima trend over  
32 time. The promising results for Great Britain support the aspiration that continuous  
33 simulation from large-scale hydrological models, supported by the increasing  
34 availability of global weather, climate and hydrological products, could be used to  
35 develop robust methods to help engineers estimate design floods in regions with  
36 limited gauge data or affected by environmental change.

37

## 38 1. Introduction

39 An accurate estimate of the design flood, i.e. the peak flow for an assigned probability  
40 of exceedance (NERC, 1975), is a critical requirement for reducing the social and  
41 economic impact of floods. Floods constitute 40% of worldwide natural disasters (EM-  
42 DAT, 2015) and often cause fatalities and damage to houses, businesses and  
43 infrastructure. Commonly, design flows are estimated with statistical models fitted to  
44 annual maxima (AMAX) measured at a gauged site (flood frequency analysis).  
45 Unfortunately hydrological records are often unavailable at the site of interest or, when  
46 available, they are too short to allow reliable statistical analyses. To overcome this  
47 limitation a standard approach is to adopt a “regionalization” procedure which  
48 introduces data from other sites into the flood frequency analysis, chosen on the basis  
49 that they exhibit similar hydrological behaviour. The regions from which these sites

50 can be selected are typically defined using one of several different regionalization  
51 methods such as cluster analysis, the region of influence approach, the method of  
52 residuals and canonical correlation analysis. Several authors review these  
53 regionalization methods (Blöschl et al., 2013, Srinivas et al., 2008, Hrachowitz et al.,  
54 2013). The index flood method (Dalrymple, 1960) is one of the most popular  
55 regionalization procedures among engineers and practitioners (NERC, 1975; Hosking  
56 and Wallis, 2005; Institute of Hydrology, 1999). The method is based on the  
57 assumption that, for all the sites inside a “hydrologically homogeneous” region, the  
58 AMAX frequency distributions are identical apart from a local scaling factor (index  
59 flood, IF [ $\text{m}^3 \text{s}^{-1}$ ]). This assumption allows the computation of any p-th quantile at any  
60 location i-th as:

$$61 \quad Q_i^p = IF_i \cdot q^p \quad (1)$$

62 where  $IF_i$  is the index flood at location i and  $q^p$  [-] is the regional growth curve, a  
63 dimensionless quantile function assumed to be identical for all the sites in the region.  
64 Various approaches have been developed to provide reliable estimates of IF, and  
65 Bocchiola et al., (2003) provides a summary of some of the most widely used. Broadly,  
66 if the site of interest is gauged, the IF can be estimated by direct methods, i.e. from  
67 the AMAX time series, using the sample mean (Dalrymple, 1960, Hosking and Wallis,  
68 1993, NERC, 1975), the sample median (Robson and Reed, 1999), or using peak over  
69 threshold analysis (Chow et al., 1988, Robson and Reed, 1999). If the site of interest  
70 is ungauged, a variety of “indirect” methods have been proposed to estimate IF. The  
71 most commonly used are empirical methods (Hirsch et al., 1992; Meigh et al., 1997;  
72 Kjeldsen and Jones, 2009) that relate the IF evaluated by AMAX measurements to a  
73 set of morpho-climatic catchment descriptors such as area, slope, average annual  
74 rainfall, land use, etc. These methods include coefficients that are usually estimated

75 by least squares (e.g. Stedinger and Tasker, 1985), maximum-likelihood (e.g. Kjeldsen  
76 et al., 2008), and Bayesian methods (e.g. Haddad et al., 2012). The uncertainty in the  
77 IF estimate attributable to the data used in the regression model calibration was  
78 quantified by Jaafar, W., Zurina and Han, (2012). Other indirect approaches for  
79 estimating IF and flow quantiles are based on the use of artificial neural networks  
80 (e.g. Hall et al., 2002; Shu and Burn, 2004; Dawson et al., 2006) or on the connection  
81 between stochastic rainfall models and lumped flow routing models (Cordova and  
82 Rodriguez Iturbe, 1983; Brath et al., 1992; Calver et al., 2005; Kjeldsen et al., 2005;  
83 Rigon et al., 2011). Limitations of the latter modelling approach are: i) the simplified  
84 assumptions for the hydrological model component; ii) the requirement of catchment  
85 initial moisture conditions; iii) the assumption of high simplified and uniform rainfall  
86 storms in catchment.

87 Indirect estimation of IF based on continuous physically-based hydrological model  
88 simulations has also been explored in recent years. The advantages of such an  
89 approach include: i) taking into account catchment heterogeneity, ii) accommodation  
90 of temporal and spatial rainfall variability, and iii) ability to provide a consistent IF  
91 estimate for multiple points on the river network. Demonstrations of the use of  
92 continuous, physically-based model simulations for flood frequency analysis are  
93 provided for various catchments by Cameron et al., (2000), Calver et al., (2005),  
94 Moretti and Montanari, (2008), and Viviroli et al., (2009)., but to our knowledge, only  
95 Ravazzani et al., 2015 used continuous hydrological model simulation for estimating  
96 the IF. They applied the model FEST-WB (Montaldo et al. 2007, Rabuffetti et al. 2008)  
97 to reconstruct river flows for an alpine basin in the north part of Italy and to predict the  
98 IF.

99 For a gauged location, an estimate of the IF recommended by the FEH, is the median  
100 of the observed AMAX. This corresponds to the 2 year return period flow which is  
101 considered a good estimate of the bankfull river discharge. If less than 14 years of  
102 AMAX are available, the FEH suggests use of peak over threshold data. For ungauged  
103 sites, the Environment Agency Flood Estimation Guidelines 2012 recommends use of  
104 the regression model of Kjeldsen et al. (2008) to estimate the IF. Practitioners are also  
105 advised that data transfer from donor catchments to the site of interest can improve  
106 the accuracy of IF estimates (Kjeldsen and Jones, 2007). The “donors” are gauged  
107 catchments hydrologically similar to the site of interest (i.e. located upstream or  
108 downstream on the same river, or possessing similar size and land use).

109 Here we present a general methodology to estimate the IF at national scale using  
110 continuous hydrological simulation (Section 2). This approach aims to: i) integrate the  
111 indirect methods for IF estimation and address their limitations for larger and spatially  
112 heterogeneous catchments, and ii) provide effective tools for IF estimation in  
113 ungauged or poorly gauged catchments. The methodology is tested in Great Britain  
114 (Section 3) and assessed (Section 4) by comparison with estimates of the IF at 550  
115 gauging stations.

116

## 117 2. Methodology

118 The area-wide physically-based hydrological model Grid-to-Grid (G2G, Bell et al.,  
119 2007a,b; 2009) has been used to estimate the IF at national scale. The G2G typically  
120 operates at a 1km<sup>2</sup> resolution across Britain and has been configured to represent  
121 spatial variability in catchment response. The model uses landscape information  
122 provided by gridded spatial datasets of elevation, soil and geology in preference to the  
123 identification of model parameters through catchment calibration, and for the

124 application discussed here, a single model configuration and set of parameters is  
125 applied across Britain (i.e. with no catchment calibration). G2G model configuration  
126 and inputs are discussed in subsection 2.1. Model output consisting of river flow time  
127 series at each 1km<sup>2</sup> river grid-cell are used to construct maps of AMAX across Britain  
128 and to estimate the IF following the FEH methodology (Institute of Hydrology, 1999).  
129 Annual maxima in the UK are taken as the highest flow value recorded in a water year,  
130 which runs from October to September.

131 G2G modelled IFs were compared to measured IFs for 550 gauged sites using  
132 observations obtained from the National River Flow Archive (NRFA). Modelled and  
133 measured IFs were compared using a linear regression, together with an analysis of  
134 the sensitivity of model performance to morpho-climatic catchment descriptors. The  
135 agreement between the G2G-derived and the measured IF was evaluated by: i)  
136 quantifying the coefficient of determination, and ii) assessing the uncertainty in IF  
137 estimate using the factorial standard error (Kjeldsen, 2014). Maps of model residuals  
138 (differences between modelled and measured IF) provide additional information on  
139 regions and types of catchment where the model performs best (and worst). Finally  
140 the temporal trends of modelled and measured AMAX were compared to assess the  
141 model capability in detecting observed long term trends.

142

## 143 2.1 Grid-to-Grid model set-up and input data

144 The Grid-to-Grid Model (Bell et al., 2007a) is a grid-based hydrological model that  
145 simulates surface and sub-surface runoff, lateral movement of soil-moisture, and flow-  
146 routing along rivers. Over Britain it is typically applied at a 1km<sup>2</sup> grid resolution and a  
147 15-minute time-step, and is configured using spatial datasets of topography, soil, and  
148 land cover. Applications include flood forecasting (e.g. Cole and Moore, 2009) and

149 assessment of climate change impacts on floods and snowmelt (i.e. Bell et al., 2007b;  
150 Bell et al., 2009; Bell et al., 2016). The most recent version of the model as presented  
151 in Bell et al., (2016) was tested over the Great Britain for the period 1960-2011. Driving  
152 data consist of daily precipitation observations on a 1 km<sup>2</sup> grid, (CEH GEAR: Keller et  
153 al., 2015), monthly PE estimates on a 40 km<sup>2</sup> grid (MORECS: Hough and Jones,  
154 1997), and daily minimum and maximum temperature observations on a 5km<sup>2</sup> grid for  
155 1960–2014 (Perry et al., 2009) which were applied through the day using a sine curve  
156 and downscaled to 1 km<sup>2</sup> using a lapse rate and elevation data (Morris and Flavin,  
157 1990). Model output consisting of 15 minutes river flows were used to provide AMAX  
158 values for 1km<sup>2</sup> river grid-cells across Britain.

159

### 160 3. Study Area and Data Availability

161 The study region includes 550 catchments from England, Scotland, and Wales. They  
162 are part of the United Kingdom peak flow dataset (version v4.1) obtained from “The  
163 National River Flow Archive” (NRFA, 2008; Dixon et al., 2013) and available at  
164 <http://nrfa.ceh.ac.uk/>. For the purposes of this analysis we used the instantaneous  
165 peak flow AMAX values and a set of catchment descriptors consisting of: the  
166 catchment area (AREA [km<sup>2</sup>]); the average annual rainfall (SAAR, [mm]) for the period  
167 1961-1990; the base flow index based on the Hydrology Of Soil Types classification  
168 presented in Boorman et al., 1995 (BFIHOST [-]), which reflects the geology of the site  
169 and has typical values that ranges from below 0.2 (highly impermeable) to above 0.8  
170 (highly permeable); the mean distance between each pixel of the basin and the outlet  
171 (mean drainage path length, DPLBAR, [km]), and the extent of urban and suburban  
172 land cover during the year 2000 (URBEXT2000, [-]). Table 1 summarises these  
173 catchment properties in terms of the mean, minimum, maximum, and standard



174 deviation value over the chosen set of 550 catchments. Of the 810 catchments for  
175 which peak flow data are available in Great Britain, 260 have been excluded for various  
176 reasons, including catchment size, and how well the gauged flows are thought to  
177 represent actual flows. Specifically, 225 catchments where  $DPLBAR < 10$  km and Area  
178  $< 50$  km<sup>2</sup> have been excluded from the comparison of simulated and observed peak  
179 flows as modelled flows for these relatively small catchments were most likely to be  
180 adversely affected (underestimated) by the use of daily mean rainfall. These  
181 catchments have a faster hydrological response and probably the use of hourly rainfall  
182 data would be more appropriate to mimic the instantaneous peak flows. A modest  
183 number of catchments (35) were excluded due to strong anthropogenic influences  
184 including: i) the presence of an artificial channel that modifies the natural flow-paths;  
185 ii) unreliable rating curves due to the lack of high flow measures; and iii) strong  
186 influence of reservoirs or groundwater abstraction on the flow regime. Figure 1  
187 presents a map of the study area, the location of the gauges selected for the analysis  
188 (black points), and the excluded gauges (white points).

189

## 190 4 Results and Discussion

### 191 4.1 Model Verification and Index Flood Map Estimation

192 A linear regression model was fitted to the measured and modelled log-transformed  
193 IF values for 550 catchments. The G2G model was executed for the whole simulation  
194 period (1960-2014) and the modelled IF in a given gauged station was computed using  
195 the modelled AMAX values corresponding to the period for which the measurements  
196 were available. Figure 2-a shows a scatterplot of 550 G2G and observation-derived  
197 IFs in logarithm scale, together with the derived linear regression model plot, and  
198 Table 2 shows the summary statistics of the linear regression model. The high values

199 of the t-ratio, computed as the coefficient estimated value divided by its estimated  
200 standard deviation, give an indication that the estimated coefficients are statistically  
201 different from 0. The coefficient of determination  $R^2=0.91$  summarizes the goodness  
202 of fit. Following Kjeldsen (2014), given the large number of catchments for which the  
203 model was evaluated (550) it is reasonable to assume that the prediction variance can  
204 be approximated by the variance of the regression model residuals,  $s=0.15$ . Under this  
205 assumption it is possible to evaluate the factorial standard error of the model  
206  $FSE=1.47$ . The latter defines the 68% and 95% confidence intervals for the regression  
207 model as  $[q \cdot FSE^{-1}; q \cdot FSE]$  and  $[q \cdot FSE^{-2}; q \cdot FSE^2]$  respectively (Kjeldsen, 2014),  
208 where  $q$  indicates given discharge value. In our case  $q$  corresponds to the median of  
209 the AMAX. The FSE presented in this study is comparable with the FSE values of the  
210 regression models currently used in FEH which are based on the AMAX  
211 measurements of 600 gauging stations. The original FEH index flood regression model  
212 reported an FSE value of 1.56 (Robson and Reed, 1999) and the revised model  
213 lowered it to 1.431 (by assuming that the correlation between model errors is a function  
214 of the geographical distances between gauging stations (Kjeldsen et al., 2008)).  
215 Figure 2-b presents a map of the residuals between modelled and measured IF using  
216 a logarithmic scale. The residuals are close to zero across most of Britain, with a  
217 modest underestimation in central and south west England, and a similarly modest  
218 overestimation in the South East. A significant factor contributing to the  
219 underestimation is the contribution of short-duration intense rainfall events to peak  
220 river flows in central and southern Britain, which will be poorly represented by daily  
221 gridded rainfall observations, while the overestimation in southern and eastern Britain  
222 can, for many groundwater-dominated catchments, be attributed to the effects of  
223 artificial abstractions which are not currently included in the G2G model formulation.

224 Figure 3-a presents a map of the modelled index flood ( $\text{m}^3\text{s}^{-1}$ ) on a logarithmic scale,  
225 for the period 1960 to 2014. The IF is typically higher in the north and west of Britain,  
226 and in major rivers. The use of continuous G2G model simulation provides a consistent  
227 spatial and temporal dataset to explore whether there has been a significant change  
228 in the IF over the last 50 years. Figure 3-b presents a map of the change in the derived  
229 index floods between two periods: 1960 to 1986 and 1987 to 2014. The changes range  
230 from an increase in the IF of up to  $45 \text{ m}^3\text{s}^{-1}$  (predominantly in the north and west) to a  
231 decrease of  $-40 \text{ m}^3\text{s}^{-1}$  in parts of Southeast Britain. This regional split is broadly in line  
232 with the increased trends detected in measured mean daily flows since the early 1960s  
233 in Scotland and, to a lesser extent, Wales and western England (Hannford and Marsh,  
234 2008). However, the authors noted that the analysis of trends in some areas was  
235 limited by the available length of record.

236 The use of continuous model simulation provides a method of estimating the IF with a  
237 91% agreement with observation-derived estimates for 550 catchments across Britain.  
238 In order to investigate whether this agreement is influenced by catchment properties  
239 a series of analyses relating model fit with properties such as area, drainage path  
240 length, urban extent and baseflow index were undertaken. For each catchment  
241 property, the catchment values were divided into deciles (i.e. the nine values that  
242 divide the sorted data into ten equally sized subsamples) and measured and modelled  
243 IF for each catchment property subgroup were compared. Figure 4 presents 10  
244 scatterplots and the coefficient of determination ( $R^2$ ) of linear models fitted to the  
245 results for the catchment property: AREA. The title of each scatterplot specifies the  
246 AREA range [ $\text{km}^2$ ] of each classes, for example the first plot is for catchments which  
247 range in area from 53 to 80  $\text{km}^2$ , the second from 80 to 110  $\text{km}^2$ , etc. Similar results  
248 are presented for percentage of urban extent (URBEXT2000) in Figure 5, and for

249 baseflow index (BFIHOST), and drainage path length (DPLBAR) in Figure A1 and A2  
250 in Appendix 1. The model fit is robust in the sense that is not strongly affected by the  
251 catchment properties. The decile range in  $R^2$  is 0.82-0.90 for AREA, 0.78-0.92 for  
252 URBEXT2000, 0.81-0.93 for BFIHOST, and 0.84-0.91 for DPLBAR. These figures  
253 indicate relatively high levels of agreement between modelled and measured IF  
254 estimates, suggesting that the quality of the G2G estimated IF is relatively unaffected  
255 by different catchment properties and can provide estimates of consistent quality  
256 across various types of catchment (e.g. small, steep, or urbanized catchments).

257

#### 258 4.2 Annual Maxima Trend Analysis

259 In the previous section we assessed whether AMAX output from a G2G continuous  
260 simulation could be used to estimate the measured IF by comparing the median of  
261 observed and simulated AMAXs over several decades. Typically, however, climate,  
262 anthropogenic or natural changes at the catchment scale can lead to long-term trends  
263 in observed annual maxima. For this reason it is important to ensure that if AMAX from  
264 continuous hydrological simulation are used in place of observed AMAX, they can also  
265 reproduce observed trends in river flows. This trend analysis has now been  
266 undertaken on 285 catchments, selected from the original 550, for which at least 40  
267 year of measured flow data are available and the Mann Kendall test (MK, Kendall,  
268 1975) with permutations provides a measure of the significance of potential trends in  
269 time. This method is presented in detail by Kundzewicz and Robson (2000) and has  
270 been used in several applications (i.e. Hannaford and Marsh, 2008, Hannaford and  
271 Marsh, 2006). The procedure is as follows: i) randomly re-order the AMAX time series  
272 to provide a large number of samples with no replacement; ii) perform Mann-Kendall  
273 trend test to each sample; iii) rank the trend test results; iv) compute the trend test for

274 the original time series. If the derived trend for the original series falls outside the [0.05,  
275 0.95] percentile range of the ranked values, it is deemed to be significant at the 95%  
276 confidence level, indicating a change in the magnitude of the AMAX over the 40-year  
277 period. The statistical tests have been performed on both measured and modelled  
278 AMAX providing test values (including the direction of the trend) and significance  
279 assessments for a trend in both the measured and modelled series. Results have been  
280 compared for the 69 catchments where the trend for the measured AMAX presented  
281 a significant test at the 95% significance level and are shown in Figure 6. No results  
282 are available for Scotland because the two criteria of at least 40 year of measured flow  
283 data are available and trend with a 95% significance level were not matched.

284 Figure 6 shows that: i) for 59 catchments positive trends were detected in both  
285 modelled and measured AMAX and ii) for 10 catchments the trend in the modelled  
286 series is not in agreement with the direction of the trend in the measured AMAXs  
287 series. These catchments are predominantly located in the south east part of England  
288 and for all of them the NRFA archive suggests that the runoff is affected by at least  
289 one of these reasons: a) reservoir in the catchment, b) presence of industrial or  
290 agricultural abstraction, and c) presence of water supply and groundwater  
291 abstractions. This anthropogenic influence which is not modelled in the current  
292 version of G2G may potentially explain the differences between measured and  
293 modelled AMAX trend in time for those basins.

294

## 295 Conclusions

296 In this paper we demonstrate how use of continuous flow simulation by a national-  
297 scale distributed hydrological model (such as G2G) can be used to estimate key  
298 parameters such as the index flood (IF) required for flood estimation methods. The

299 comparison between index floods estimated from current (FEH) and continuous  
300 simulation methods for 550 catchments throughout Great Britain indicates a good  
301 correlation between the two methods ( $R^2=0.91$ , factorial standard error FSE=1.47).  
302 We have also demonstrated that AMAX from continuous hydrological simulation can  
303 reproduce observed trends the measured annual maxima (agreement in 90% of the  
304 analysed catchments), indicating the potential utility of the methodology for conditions  
305 of non-stationarity.

306 This initial assessment of continuous simulation from a national-scale hydrological  
307 model (G2G) for estimating the IF is encouraging and demonstrates the new method  
308 can potentially overcome current methodological limitations such as the assumption  
309 of spatially homogeneous rainfall over the catchment and climate non-stationarity.  
310 Other benefits of the proposed new method include estimation of index floods in  
311 catchments subject to anthropogenic change, which at present can only be estimated  
312 using observed flows in naturalised catchments and require a correction to take into  
313 account the extent of urbanisation. Here, the accuracy of IF estimates from G2G  
314 continuous simulation is shown to be relatively unaffected by catchment properties  
315 such as area and urban extent, indicating that the methodology is robust for a variety  
316 of catchment types, so long as the continuous hydrological simulation is able to take  
317 into account the many factors (natural and anthropogenic) affecting river flows.

318 Countries such as Britain, for which an extensive network of flow and raingauges can  
319 support existing observation-based FEH methods, provide ideal test conditions for  
320 assessing the ability of alternative model-based flood estimation methods, such as  
321 continuous simulation from large-scale hydrological models, to underpin methods for  
322 flood estimation in data-sparse regions. It is to be hoped that the increasing availability  
323 and accuracy of global weather, climate and hydrological products can be used to

324 develop a robust methodology to help engineers estimate design floods in regions with  
325 limited gauge data or affected by environmental change, potentially saving many lives.

326

327

328

329

330

331

332

333

334

335

336

337

338

339

340

341

342

#### 343 References

344

345 Bell, V. A., Kay, A. L., Jones, R. G., & Moore, R. J. (2007a). Development of a high  
346 resolution grid-based river flow model for use with regional climate model output.  
347 Hydrology and Earth System Sciences, 11(1), 532-549.

348

349 Bell, V. A., Kay, A. L., Jones, R. G., & Moore, R. J. (2007). Use of a grid-based  
350 hydrological model and regional climate model outputs to assess changing flood  
351 risk. *International Journal of Climatology*, 27(12), 1657-1671.

352

353 Bell, V. A., Kay, A. L., Jones, R. G., Moore, R. J., & Reynard, N. S. (2009). Use of soil  
354 data in a grid-based hydrological model to estimate spatial variation in changing flood  
355 risk across the UK. *Journal of Hydrology*, 377(3), 335-350.

356

357 Bell, V.A.; Kay, A.L.; Davies, H.N.; Jones, R.G.. 2016 An assessment of the possible  
358 impacts of climate change on snow and peak river flows across Britain. *Climatic*  
359 *Change*, 136 (3). 539-553. 10.1007/s10584-016-1637-x

360

361 Blöschl, G. (Ed.). (2013). *Runoff prediction in ungauged basins: synthesis across*  
362 *processes, places and scales*. Cambridge University Press.

363

364 Bocchiola, D., De Michele, C., & Rosso, R. (2003). Review of recent advances in index  
365 flood estimation. *Hydrology and Earth System Sciences Discussions*,7(3), 283-296.

366

367 Boorman, D. B., Hollis, J. M., & Lilly, A. (1995). *Hydrology of soil types: a*  
368 *hydrologically-based classification of the soils of United Kingdom*. Institute of  
369 Hydrology.

370 Brath, A., Bacchi, B., and Rossi, R., (1992) The geo-morpho-climatic derivation of the  
371 probability distribution of the flood discharge. *Idrotecnica*, 4, 183-200.

372



373 Calver, A., Crooks, S., Jones, D.A., Kay, A., Kjeldsen, T. and Reynard, N., 2005.  
374 National river catchment flood frequency method using continuous simulation.  
375 Research Report to Defra, Centre for Ecology & Hydrology, Wallingford, UK.

376 Cameron, D., Beven, K., Tawn, J., & Naden, P. (2000). Flood frequency estimation by  
377 continuous simulation (with likelihood based uncertainty estimation). *Hydrology and*  
378 *Earth System Sciences Discussions*, 4(1), 23-34.

379

380 Calver, A., Crooks, S. C., Jones, D. A., Kay, A. L., Kjeldsen, T. C., & Reynard, N. S.  
381 (2005). National river catchment flood frequency method using continuous simulation.

382 Chow, V. T., Maidment, D. R., & Mays, L. W. (1988). *Applied hydrology*. McGraw Hill,  
383 New York, USA.

384

385 Cole, S. J., & Moore, R. J. (2009). Distributed hydrological modelling using weather  
386 radar in gauged and ungauged basins. *Advances in Water Resources*, 32(7), 1107-  
387 1120.

388

389 Córdova, J., & Rodríguez-Iturbe, I. (1983). Geomorphoclimatic estimation of extreme  
390 flow probabilities. *Journal of Hydrology*, 65(1), 159-173.

391

392 Dalrymple, T. (1960) Flood frequency analysis. Water Supply Paper 1543-A, US Geol.  
393 Survey, Reston, Virginia, USA

394

395 Dawson, C. W., Abrahart, R. J., Shamseldin, A. Y., & Wilby, R. L. (2006). Flood  
396 estimation at ungauged sites using artificial neural networks. *Journal of Hydrology*,  
397 319(1), 391-409.

398

399 Dixon, H., Hannaford, J., & Fry, M. J. (2013). The effective management of national  
400 hydrometric data: experiences from the United Kingdom. *Hydrological Sciences*  
401 *Journal*, 58(7), 1383-1399.

402

403 EM-DAT (2015). EM-DAT: The OFDA/CRED international disaster database —  
404 [www.emdat.be](http://www.emdat.be). Université Catholique de Louvain (Retrieved b <http://www.emdat.be/>  
405 Access 10/04/16)

406

407 FEH (1999) Flood Estimation Handbook. Institute of Hydrology, Wallingford, UK.

408

409 Shu, C., & Burn, D. H. (2004). Artificial neural network ensembles and their application  
410 in pooled flood frequency analysis. *Water Resources Research*, 40(9).

411

412 Haddad, K., A. Rahman, and J. R. Stedinger (2012), Regional flood frequency analysis  
413 using Bayesian generalized least squares: A comparison between quantile and  
414 parameter regression techniques, *Hydrol. Processes*, 26, 1008–1021

415

416 Hall, M. J., Minns, A. W., & Ashrafuzzaman, A. K. M. (2002). The application of data  
417 mining techniques for the regionalisation of hydrological variables. *Hydrology and*  
418 *Earth System Sciences Discussions*, 6(4), 685-694.

419

420 Hannaford, J., & Marsh, T. (2006). An assessment of trends in UK runoff and low flows  
421 using a network of undisturbed catchments. *International Journal of Climatology*,  
422 26(9), 1237-1253.

423

424 Hannaford, J., & Marsh, T. J. (2008). High-flow and flood trends in a network of  
425 undisturbed catchments in the UK. *International Journal of Climatology*, 28(10), 1325-  
426 1338.

427

428 Hirsch, R. M., Helsel, D. R., Cohn, T. A., Gilroy, E. J., & Maidment, D. R. (1992).  
429 Statistical analysis of hydrologic data. *Handbook of hydrology*., 17-1.

430

431 Hosking, J. R. M., & Wallis, J. R. (2005). *Regional frequency analysis: an approach*  
432 *based on L-moments*. Cambridge University Press.

433

434 Hosking, J. R. M., & Wallis, J. R. (1993). Some statistics useful in regional frequency  
435 analysis. *Water Resources Research*, 29(2), 271-281.

436

437 Hough, M. N., & Jones, R. J. A. (1997). The United Kingdom Meteorological Office  
438 rainfall and evaporation calculation system: MORECS version 2.0-an overview.  
439 *Hydrology and Earth System Sciences Discussions*, 1(2), 227-239.

440

441 Hrachowitz, M., Savenije, H. H. G., Blöschl, G., McDonnell, J. J., Sivapalan, M.,  
442 Pomeroy, J. W & Fenicia, F. (2013). A decade of Predictions in Ungauged Basins  
443 (PUB)—a review. *Hydrological sciences journal*, 58(6), 1198-1255.

444

445 Institute of Hydrology. *Flood Estimation Handbook (FEH)*, 5 Volumes. Wallingford, UK:  
446 Institute of Hydrology, 1999.

447

448 Jaafar, W., Zurina, W., & Han, D. (2012). Uncertainty in index flood modelling due to  
449 calibration data sizes. *Hydrological Processes*, 26(2), 189-201.

450

451 Kjeldsen, T. R., Stewart, E. J., Packman, J. C., Folwell, S. S., & Bayliss, A. C. (2005).  
452 Revitalisation of the FSR/FEH rainfall-runoff method. Final Report to DEFRA/EA,  
453 CEH, Wallingford.

454

455 Kjeldsen, T. R., & Jones, D. (2007). Estimation of an index flood using data transfer in  
456 the UK. *Hydrological sciences journal*, 52(1), 86-98.

457

458 Kjeldsen, T. R., Jones, D. A., & Bayliss, A. C. (2008). Improving the FEH statistical  
459 procedures for flood frequency estimation. Environment Agency.

460

461 Kjeldsen, T. R., & Jones, D. A. (2009). An exploratory analysis of error components in  
462 hydrological regression modeling. *Water resources research*, 45(2).

463

464 Kjeldsen, T. R. (2015). How reliable are design flood estimates in the UK?. *Journal of*  
465 *Flood Risk Management*, 8(3), 237-246.

466

467 Morris DG, Flavin RW (1990) A digital terrain model for hydrology. In: Proceedings of  
468 the 4th International Symposium on Spatial Data Handling, Zurich, Switzerland, 23–  
469 27 July 1990 1:250–262

470

471 Meigh, J. R., F. A. K. Farquharson, and J. V. Sutcliffe (1997), A worldwide comparison  
472 of regional flood estimation methods and climate,

473 Hydrol. Sci. J., 42(2), 225–244.

474

475 Montaldo, N., Ravazzani, G., & Mancini, M. (2007). On the prediction of the Toce  
476 alpine basin floods with distributed hydrologic models. *Hydrological processes*, 21(5),  
477 608-621.

478

479 Moretti, G. and Montanari, A., 2008. Inferring the flood frequency distribution for an  
480 ungauged basin using a spatially distributed rainfall–runoff model. *Hydrology and*  
481 *Earth System Sciences*, 12, 1141–1152. doi:10.5194/hess-12-1141-2008

482

483 National River Flow Archive (NRFA): Centre for Ecology and Hydrology, Wallingford,  
484 UK, available online: <http://nrfa.ceh.ac.uk/>, last access: 20 April 2016.

485

486 NERC (Natural Environment Research Council) (1975) Flood Studies Report. NERC,  
487 London, UK.

488

489 Perry, M., Hollis, D., & Elms, M. (2009). The generation of daily gridded datasets of  
490 temperature and rainfall for the UK. Met Office National Climate Information Centre,  
491 FitzRoy Road, Exeter, Devon EX1 3PB, UK.

492

493 Ravazzani, G., Bocchiola, D., Groppelli, B., Soncini, A., Rulli, M. C., Colombo, F., &  
494 Rosso, R. (2015). Continuous streamflow simulation for index flood estimation in an  
495 Alpine basin of northern Italy. *Hydrological Sciences Journal*, 60(6), 1013-1025.

496

497 Rabuffetti, D., Ravazzani, G., Corbari, C., & Mancini, M. (2008). Verification of  
498 operational Quantitative Discharge Forecast (QDF) for a regional warning system, the  
499 AMPHORE case studies in the upper Po River. *Natural Hazards and Earth System*  
500 *Science*, 8(1), 161-173.

501

502 Rigon, R., D'Odorico, P., and Bertoldi, G.: The geomorphic structure of the runoff peak,  
503 *Hydrol. Earth Syst. Sci.*, 15, 1853-1863, doi:10.5194/hess-15-1853-2011, 2011.

504

505 Robson, A. J., & Reed, D. W. (1999). *Flood estimation handbook*. Institute of  
506 Hydrology, Wallingford.

507

508 Srinivas, V. V., Tripathi, S., Rao, A. R., & Govindaraju, R. S. (2008). Regional flood  
509 frequency analysis by combining self-organizing feature map and fuzzy clustering.  
510 *Journal of Hydrology*, 348(1), 148-166.

511

512 Stedinger, J. R., and G. D. Tasker (1985), Regional hydrological analysis: 1. Ordinary,  
513 weighted and generalized least squares compared, *Water Resour. Res.*, 21, 1421–  
514 1432.

515

516 Viviroli, D., Zappa, M., Schwanbeck, J., Gurtz, J., & Weingartner, R. (2009).  
517 Continuous simulation for flood estimation in ungauged mesoscale catchments of  
518 Switzerland–Part I: Modelling framework and calibration results. *Journal of Hydrology*,  
519 377(1), 191-207.

520

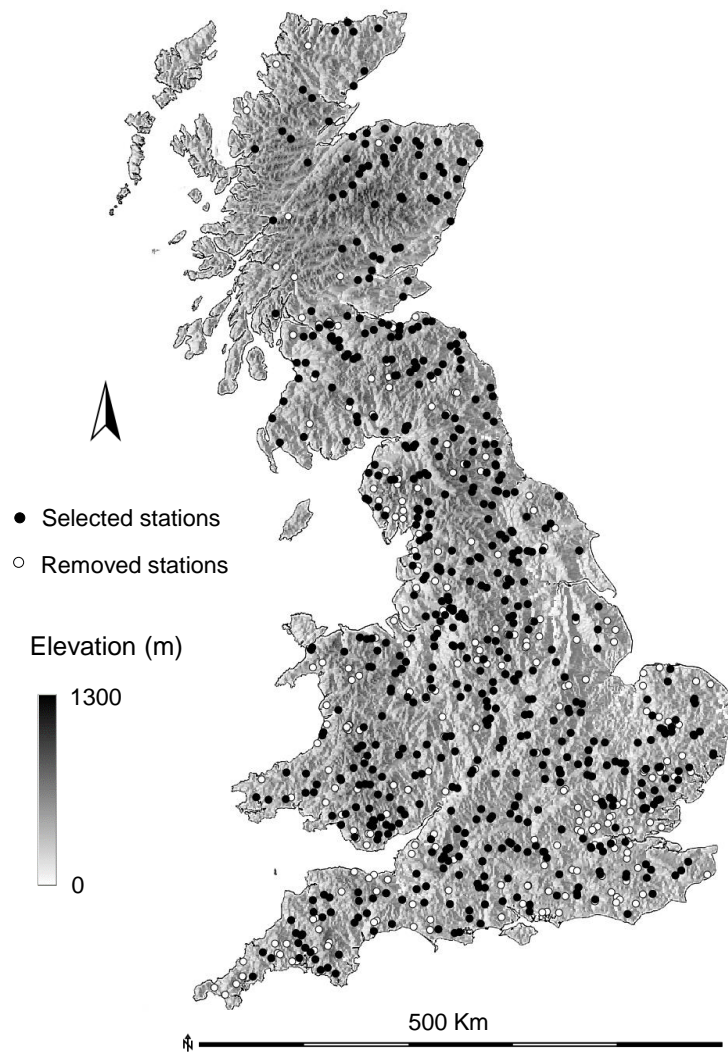
521

522

523

524 Figures

525



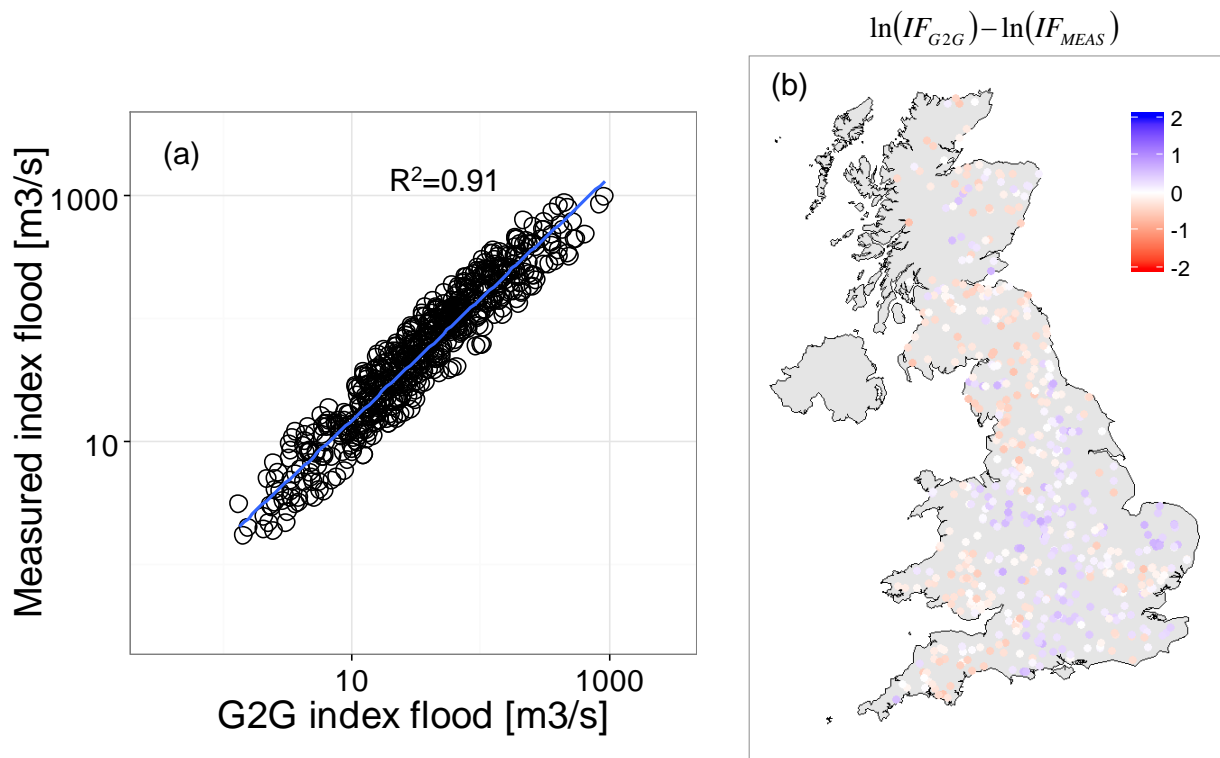
526

527 Figure 1: Location of the 550 catchments used in this study

528

529

530



531

532

Figure 2: Linear regression model (a) and residual error in logarithm scale (b) for measured and

533

modelled index floods for the 550 analysed catchments.

534

535

536

537

538

539

540

541

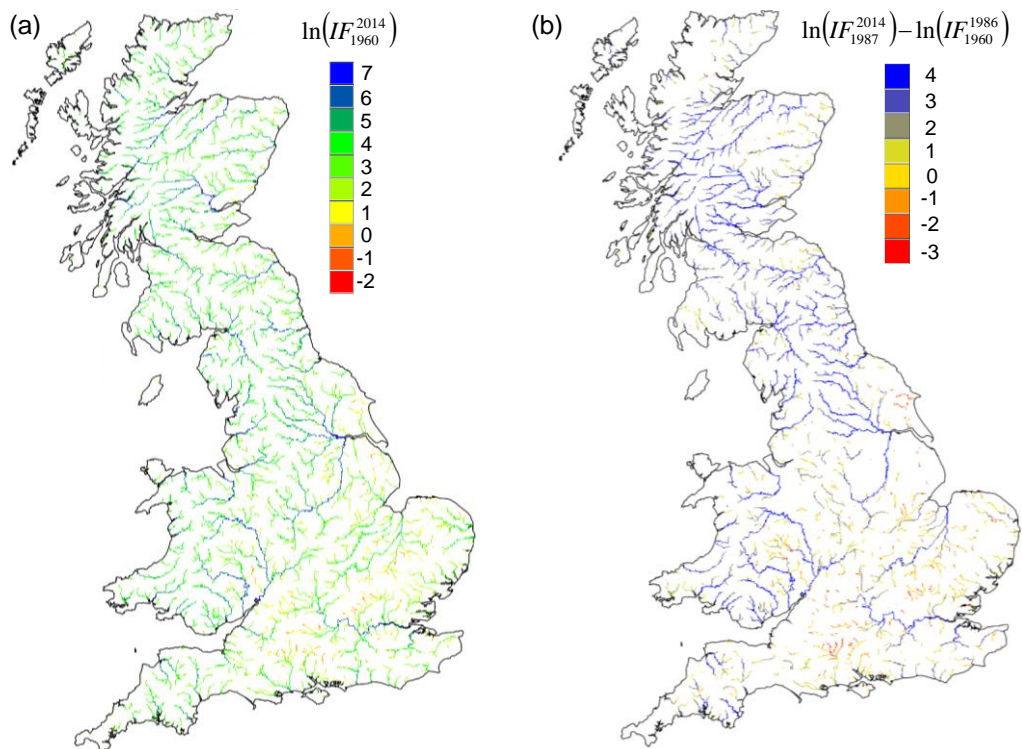
542

543

544

545





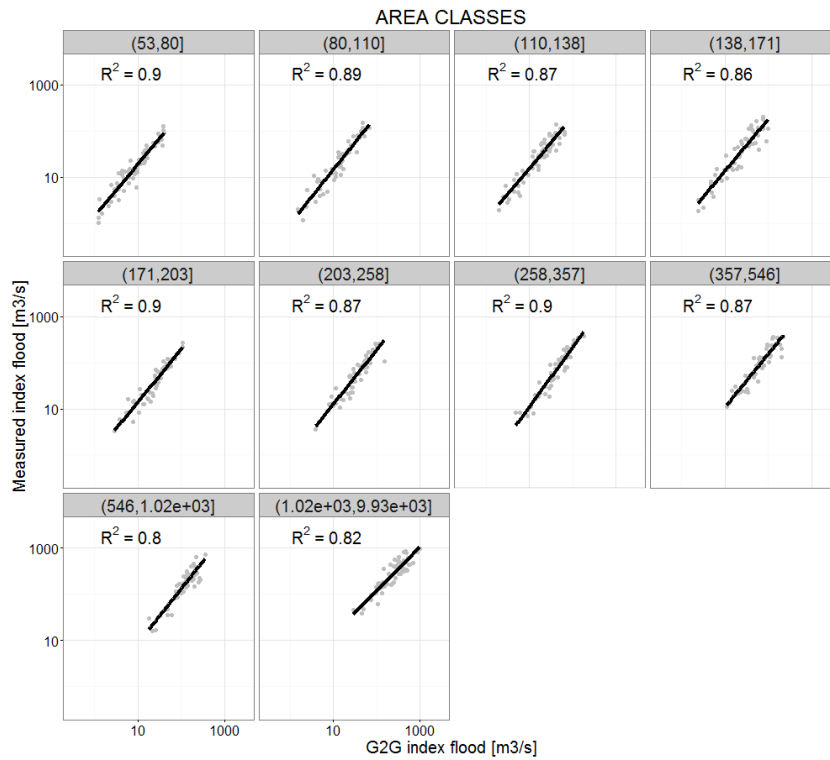
547

548 Figure 3: Maps of Britain showing, on a logarithmic scale: (a) Modelled index flood ( $\text{m}^3\text{s}^{-1}$ ) for the  
549 period 1961-2011 (b) Change in the derived index flood ( $\text{m}^3\text{s}^{-1}$ ) between 1961-1985 and 1986-2011.

550

551

552



553

554

Figure 4: Scatterplots and coefficients of determination for modelled and measured index flood

555

grouped by AREA classes.

556

557

558

559

560

561

562

563

564

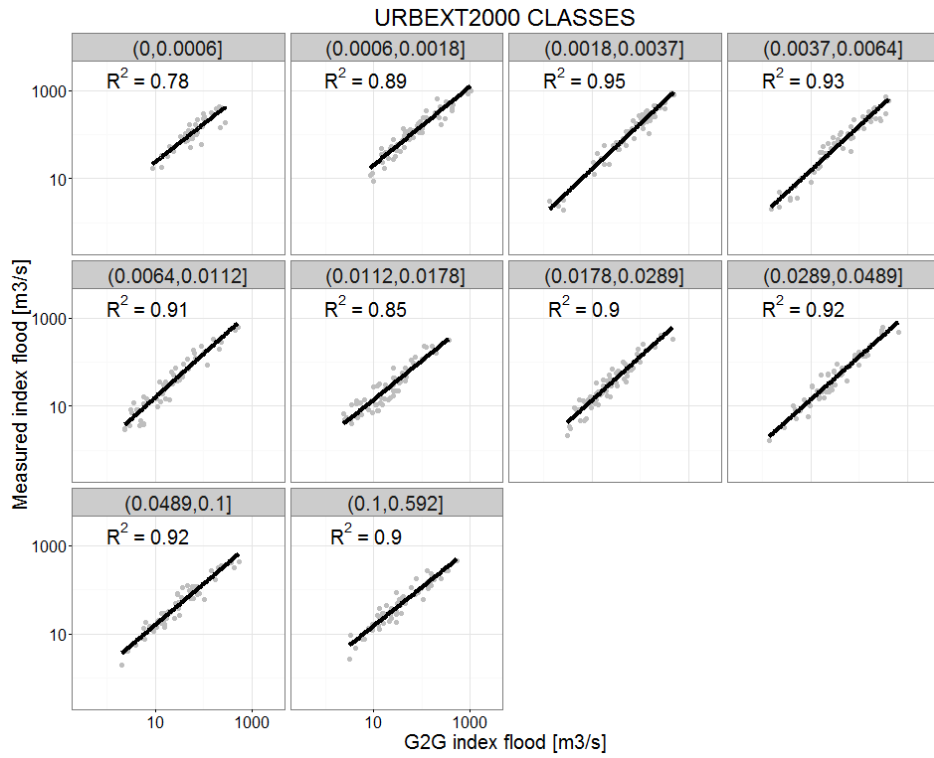
565

566

567

568

569



570

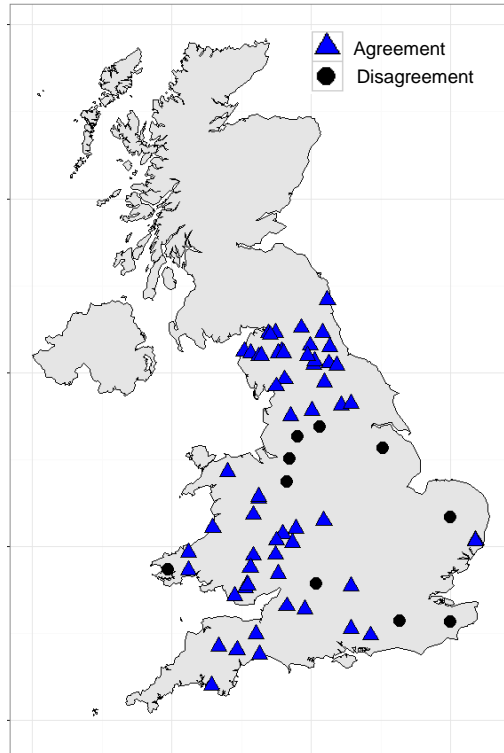
571 Figure 5: Scatterplots and determination coefficients for modelled and measured index flood grouped  
572 by URBEXT2000 classes.

573

574

575

576



577

578

579

580

581

582

583

584

585

586

587

588

589

590

591

592

Figure 6: Comparison between the measured and modelled AMAX trend with time with a 95% significance. The catchments where both model and data agree are represented by blue triangles (positive); the points where they disagree are represented by black points.

593 Tables

594

595 Table 1: Summary statistics (minimum, median, maximum, and standard deviation value) for the  
 596 selected set of catchments indicators: AREA, SAAR, BFIHOST, DPLBAR, and URBEXT2000

	AREA [km <sup>2</sup> ]	SAAR [mm]	BFIHOST [-]	DPLBAR [km]	URBEXT2000 [-]
Minimum	55	558	0.24	10	0
Median	203	962	0.47	19	0.009
Maximum	9931	2913	0.96	140	0.592
Stand. Dev.	935	401	0.14	18	0.085

597

598

599 Table 2: Summary of the linear regression model linking the measured and modelled index floods

Intercept	T-Stat intercept	Scaling exponent	T-Stat Scaling exponent	Residual Stand. Dev	R <sup>2</sup>
0.41	8.995	0.99	76.681	0.386	0.910

600

601

602

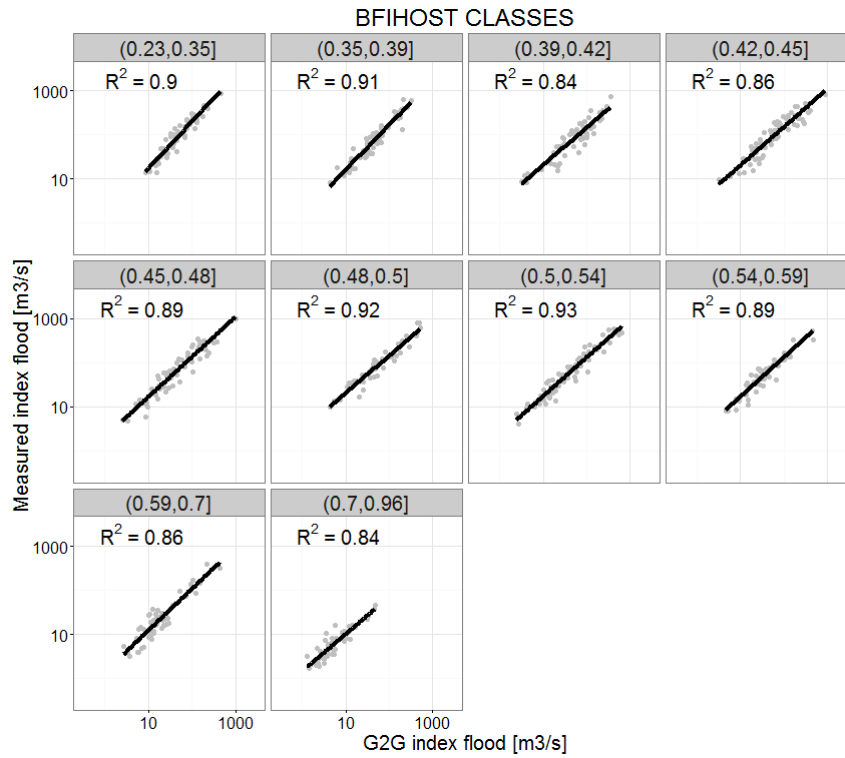
603

604

605

606 Appendix 1

607



608

609

Figure A1: Scatterplots and determination coefficients for modelled and measured index flood

610

grouped by BFIHOST classes.

611

612

613

614

615

616

617

618

619

620

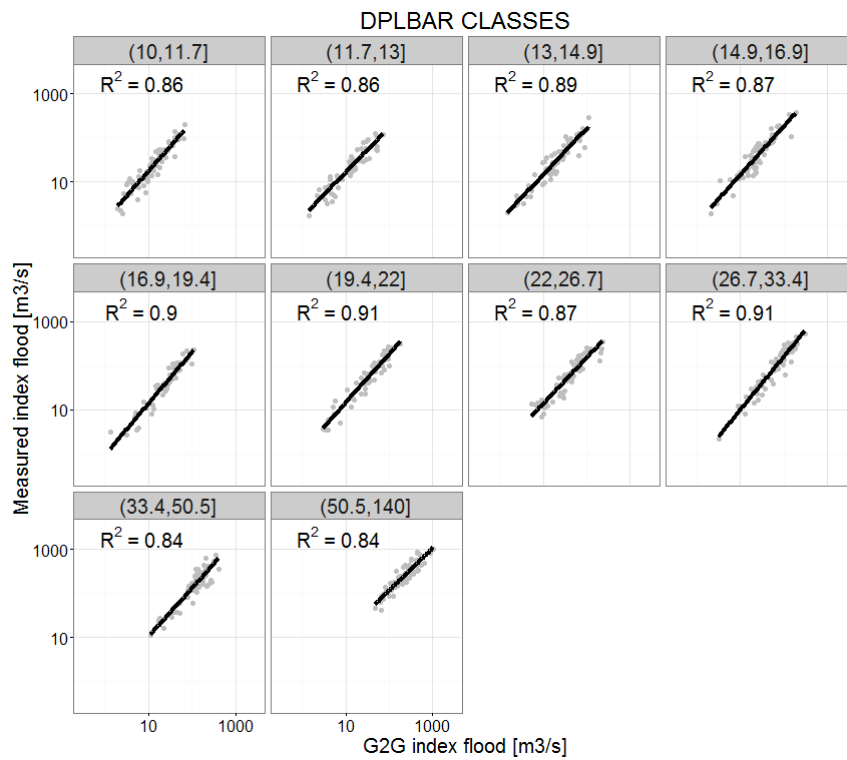
621

622

623

624

625



626

627 Figure A2: Scatterplots and determination coefficients for modelled and measured index flood

628

grouped by DPLBAR classes.